Lecture 3

Carbon nanotube

-TIGP course on nanotechnology
by Wei-Li Lee

Outline

- Structure of carbon nanotube
- Fabrication of carbon nanotube
- electronic property in carbon nanotube
- Applications of carbon nanotube

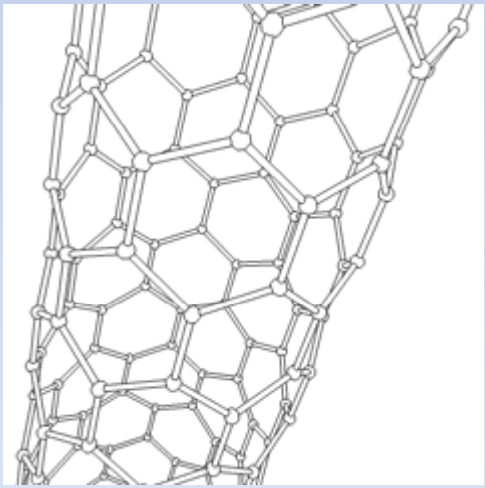

Zigzag (8,0) carbon nanotube
semiconducting

Structure of single wall carbon nanotube

Rolling of a 2-D graphene sheet

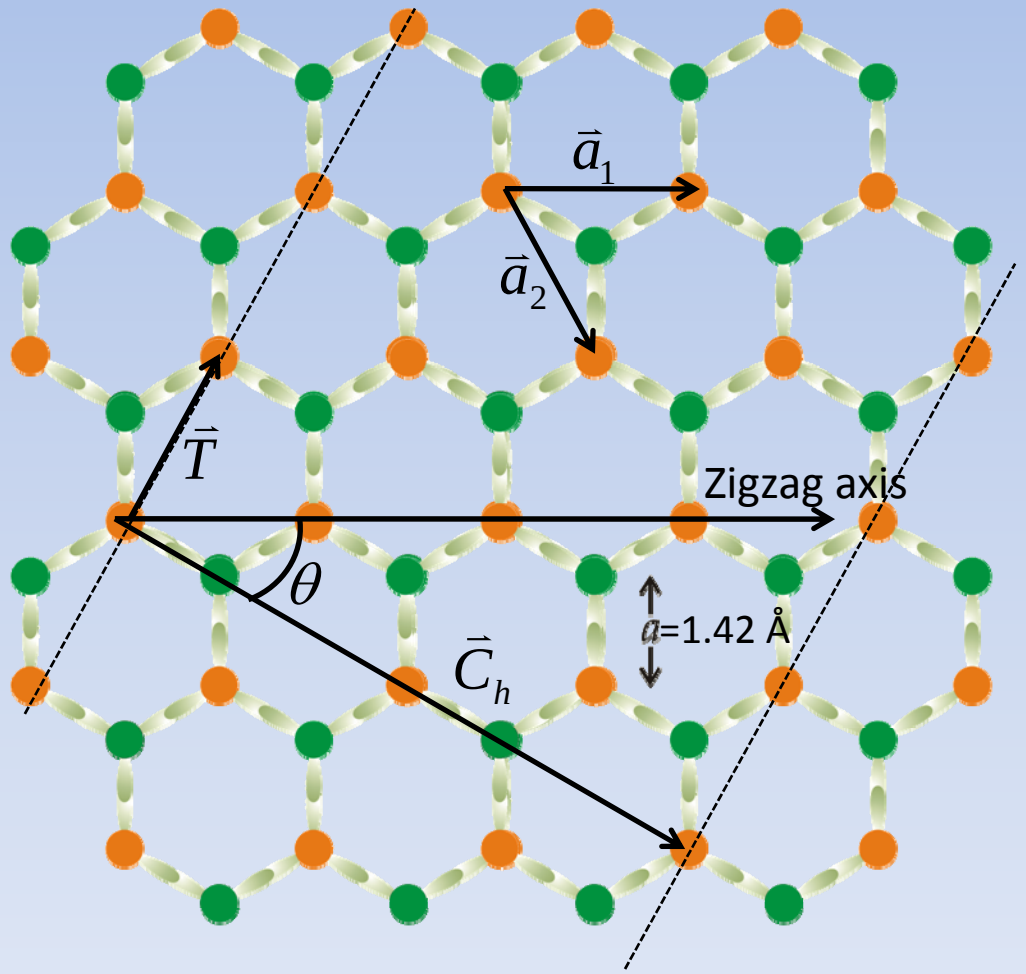

Chiral (Circumferential) vector

$$\vec{C}_h \equiv n\vec{a}_1 + m\vec{a}_2$$

Translational vector

$$\vec{T} \perp \vec{C}_h$$

Tube diameter d_t

$$d_t = \left|\vec{C}_h\right| / \pi$$

$$= \frac{a}{\pi}\sqrt{3(m^2 + mn + n^2)}$$

Angle $\theta = \tan^{-1}[\sqrt{3}m/(m+2n)]$

Rolling of a 2-D graphene sheet

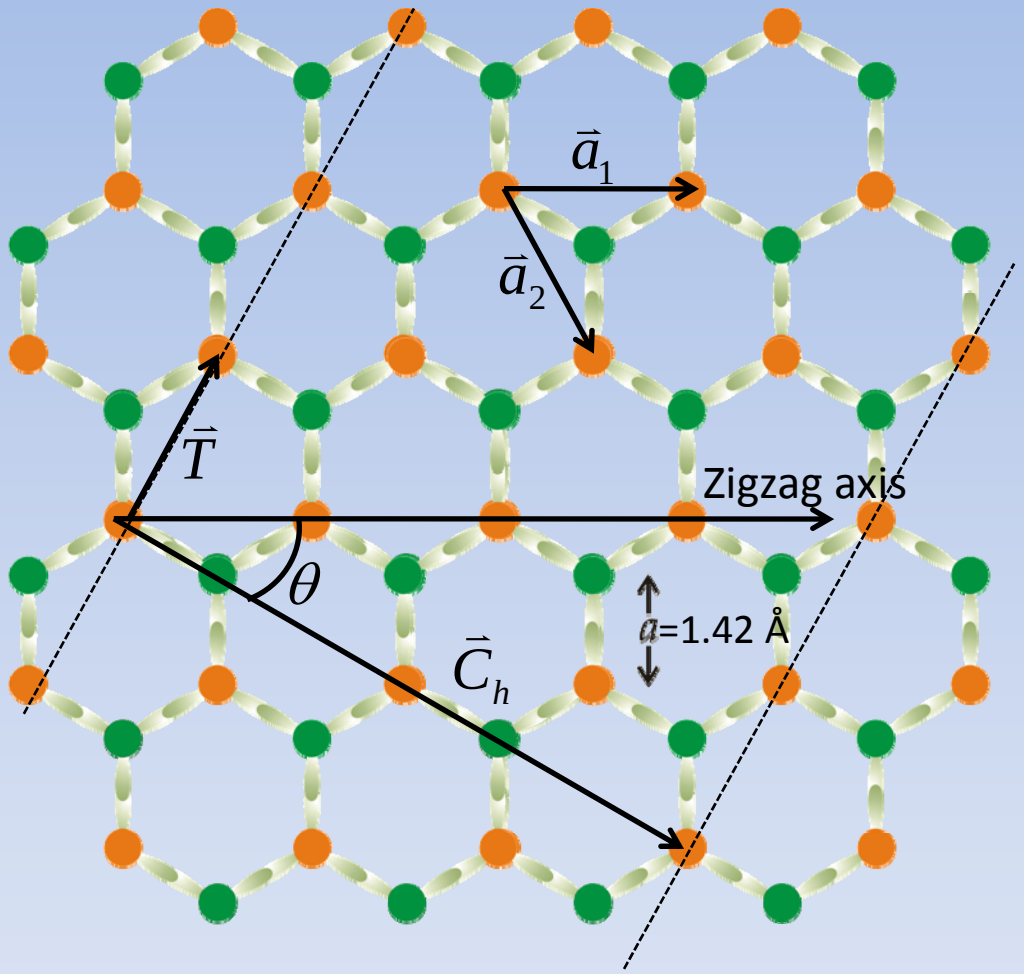

Label a carbon nanotube

$$(n, m),$$

$$where \quad \vec{C}_h \equiv n\vec{a}_1 + m\vec{a}_2$$

or

$$(d_t, \theta)$$

Tube diameter

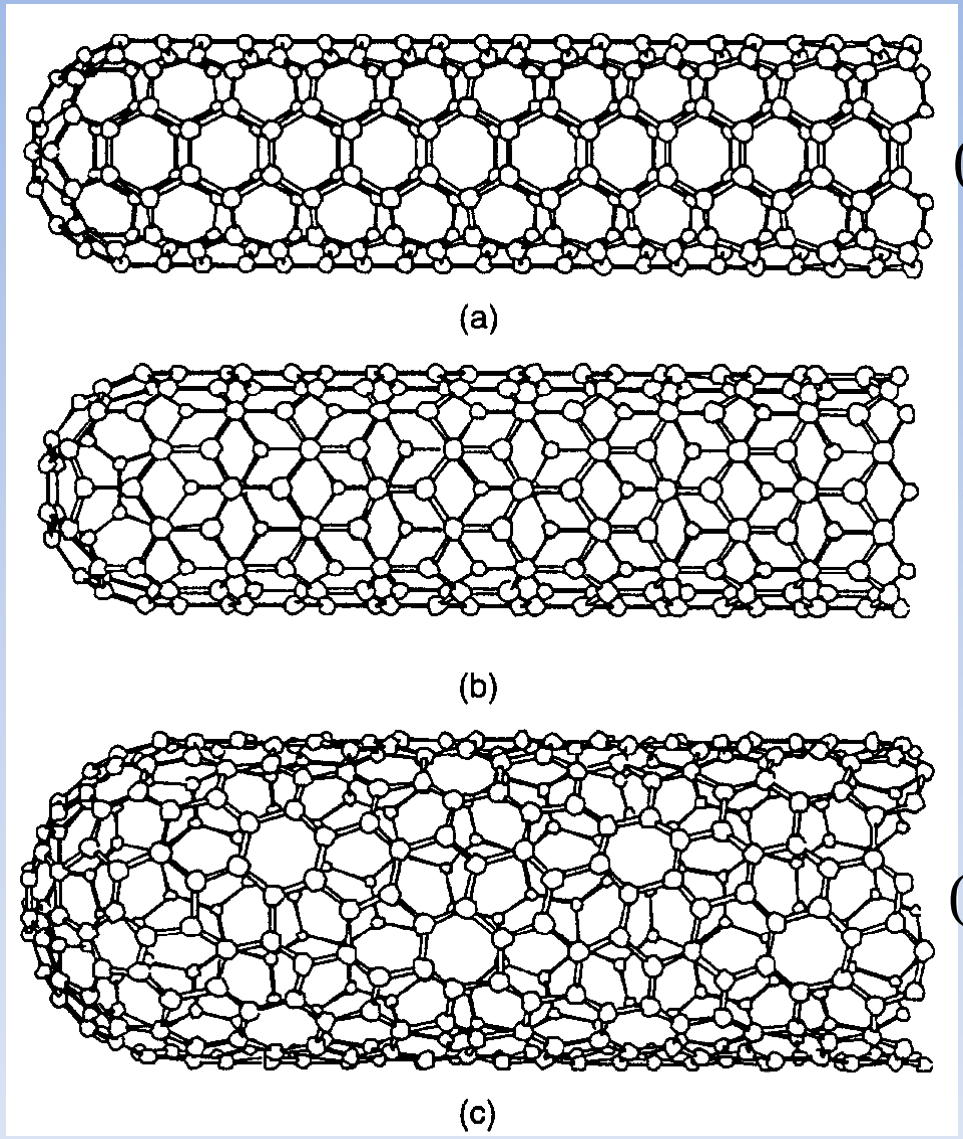

Armchair

(5,5) (n,n)

Zigzag

(9,0) $(n,0)$

Chiral

(10,5) (n,m)

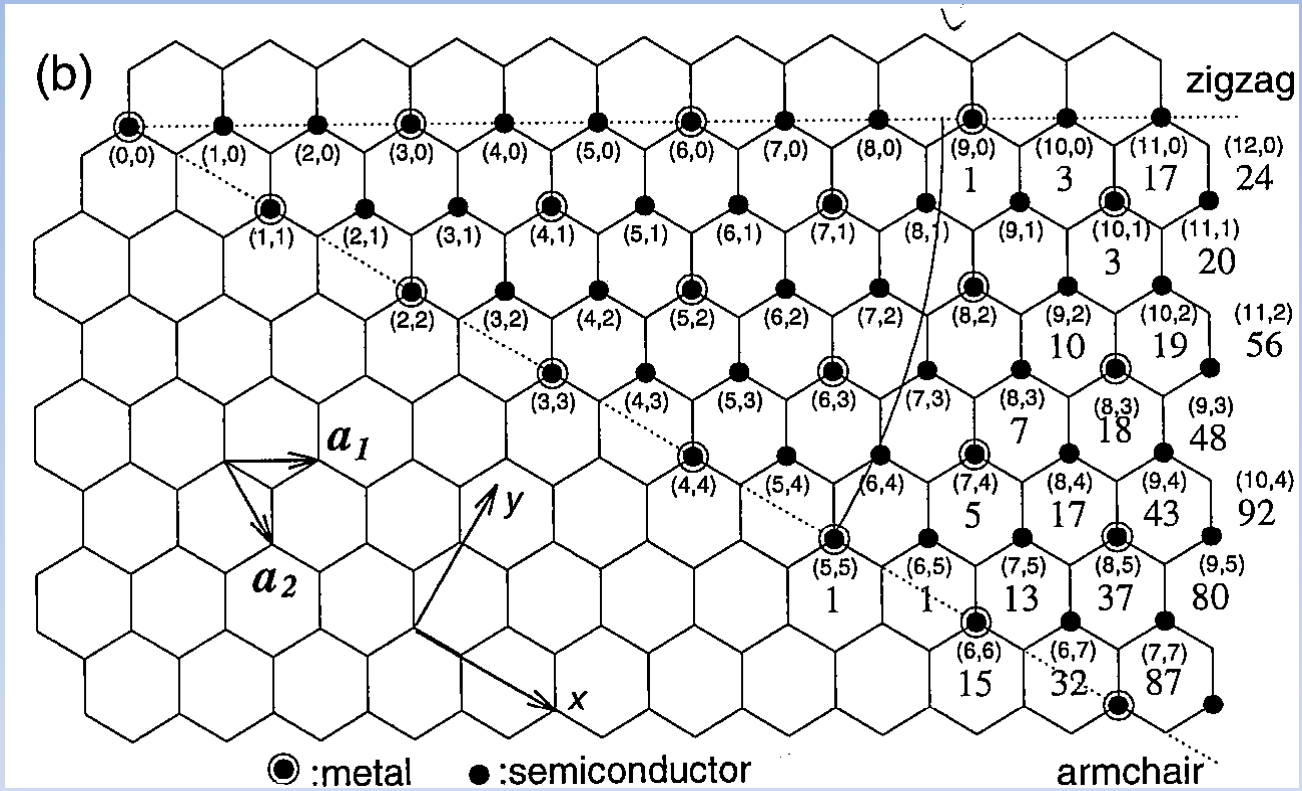

Armchair tubes are all metallic !!

Rule : metallic for n-m = 3 q , where q is an integer

Fabrication of carbon nanotube

(I) Laser evaporation

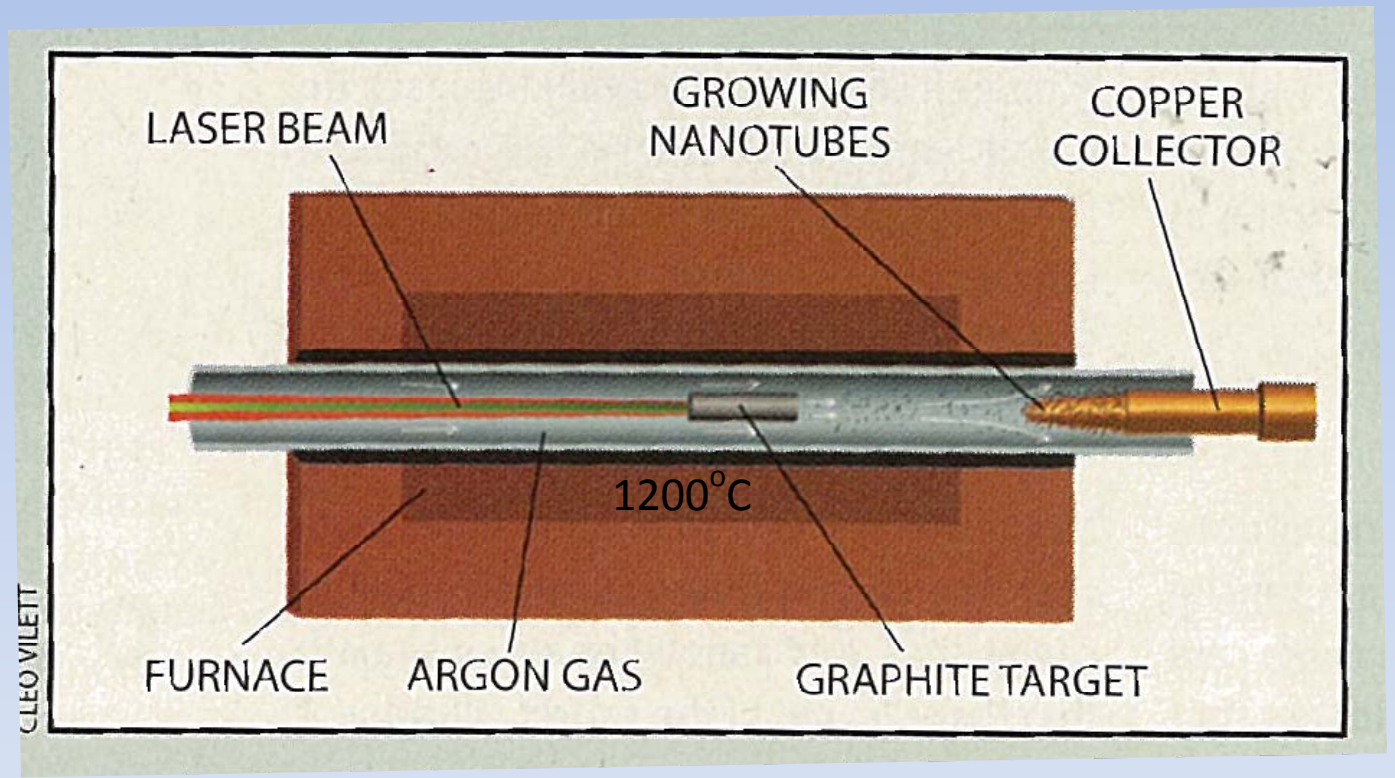

(II) Carbon arc discharging:

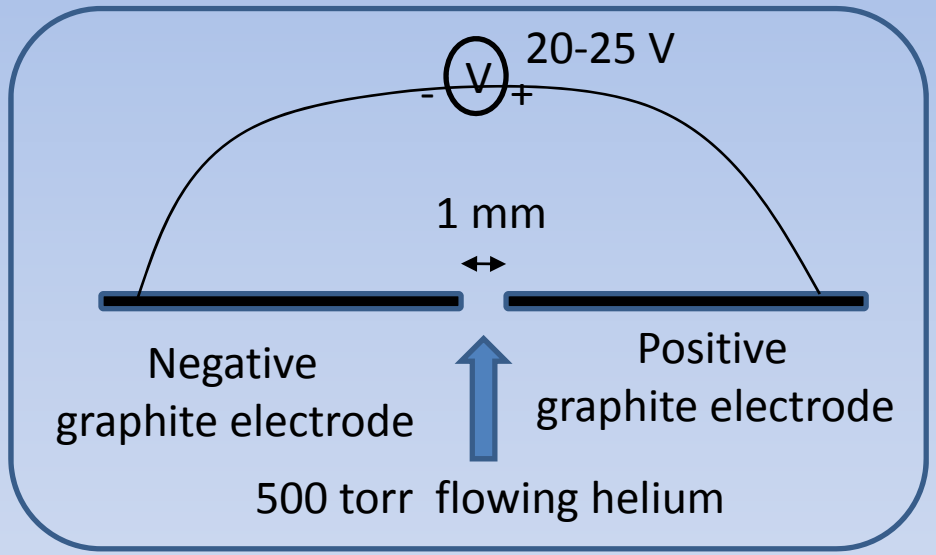

- Nanotubes (NTs) will form on the negative electrode : mostly multi-walled NTs
- Incorporate Co, Ni, Fe catalysts in the positive electrode : Single-walled NTs

(III) Plasma enhanced Chemical vapor deposition (CVD)

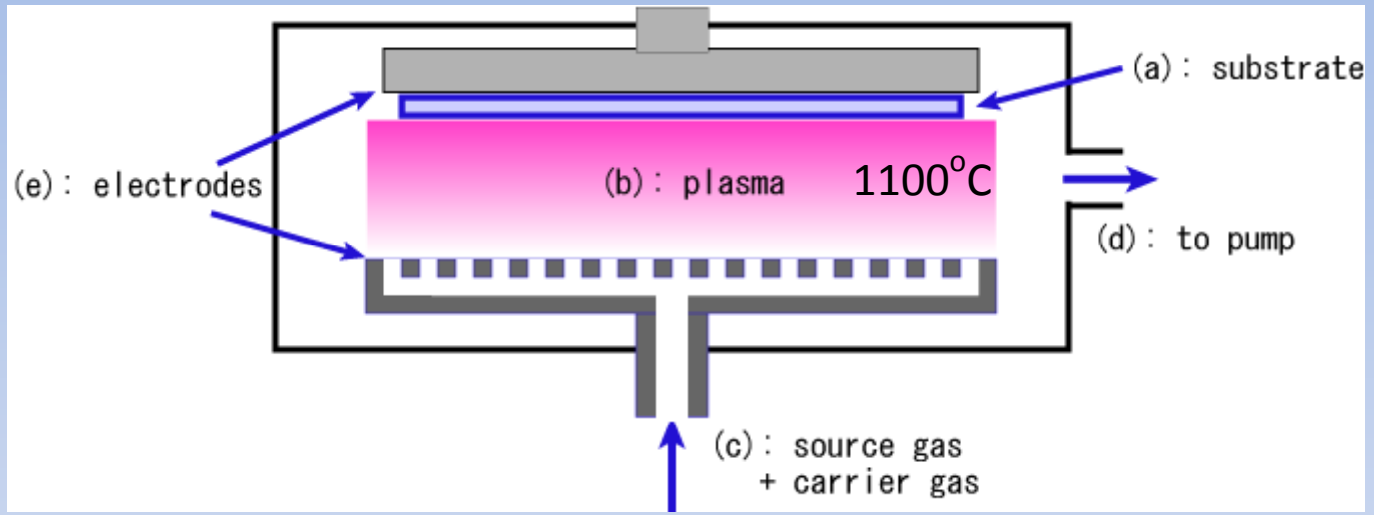

(a) Substrate : a thin layer of metal catalyst particles, Co, Ni, Fe..etc
(b) Source gas : a carbon-containing gas, CH_4, C_2H_2 …etc
Carrier gas : H_2, N_2 …etc
(c) Nanotube forms along the field direction
(d) Favorable for large scale production

Growth mechanism of carbon nanotube

(I) Not well-understood !

(II) Absorption of monomer C, dimer C_2, trimer C_3

(III) Scootter mechanism for the metal particles served as catalyst

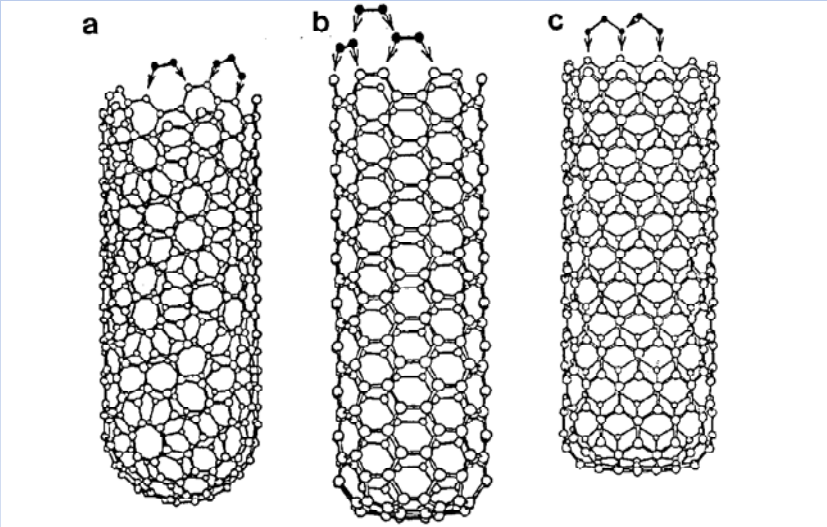

Fig. 19.21. Proposed growth mechanism of carbon tubules at an open end by the absorption of C_2 (dimers) and C_3 (trimers). (a) Absorption of C_2 dimers at the most active edge site of a chiral carbon tubule resulting in the addition of one hexagon. Also shown is an out-of-sequence absorption of a C_3 trimer. (b) Absorption of C_2 dimers at the open end of an armchair carbon tubule. (c) Absorption of a C_3 trimer at the open end of a zigzag carbon tubule and subsequent C_2 dimer absorption.

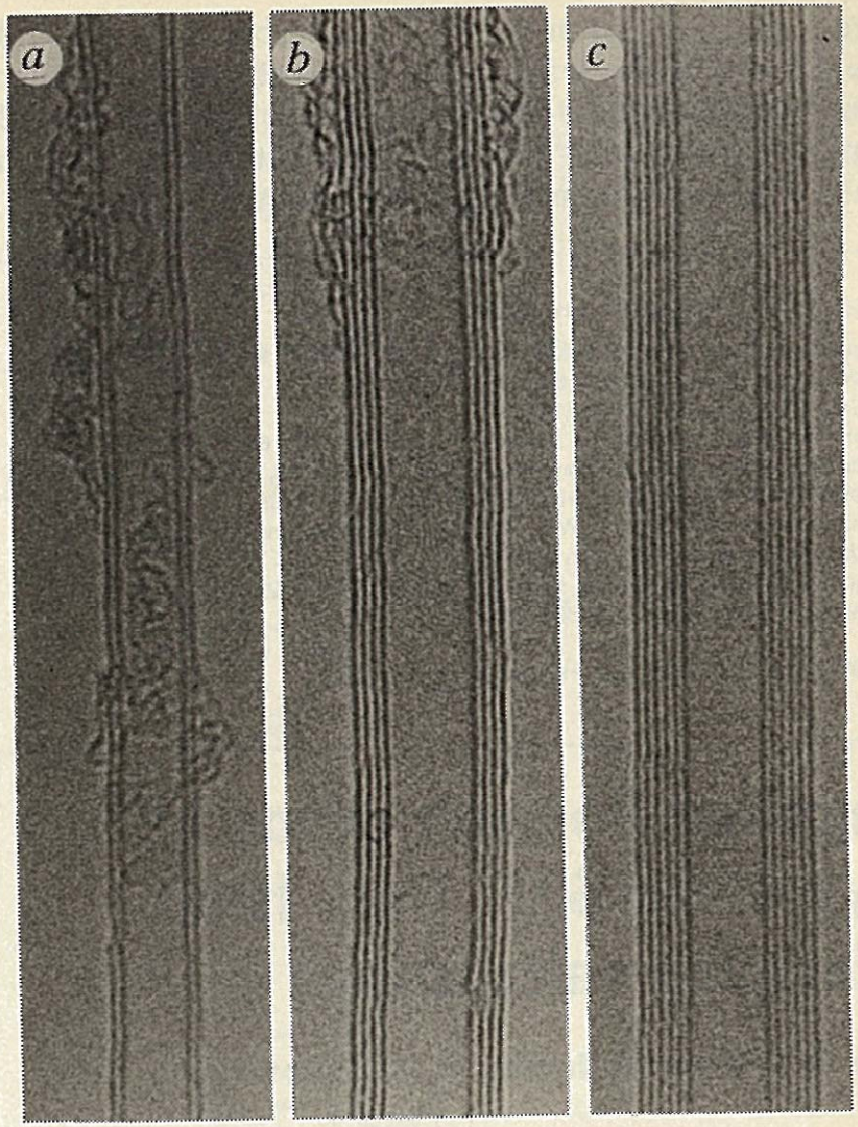

FIG. 3 High-resolution electron micrographs of typical tubes present in samples prepared under helium at 500 torr as described in the text. The number of layers ranges from two to many. The distance between consecutive carbon layers in the tubes is 0.34 nm.

Multi-Walled NTs (MWNTs):

Inter-layer distance ~0.34 nm

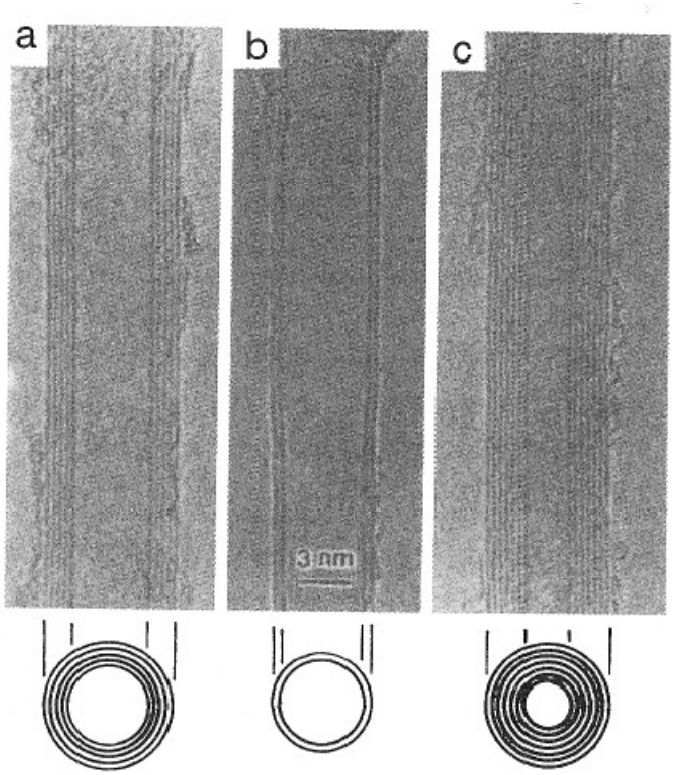

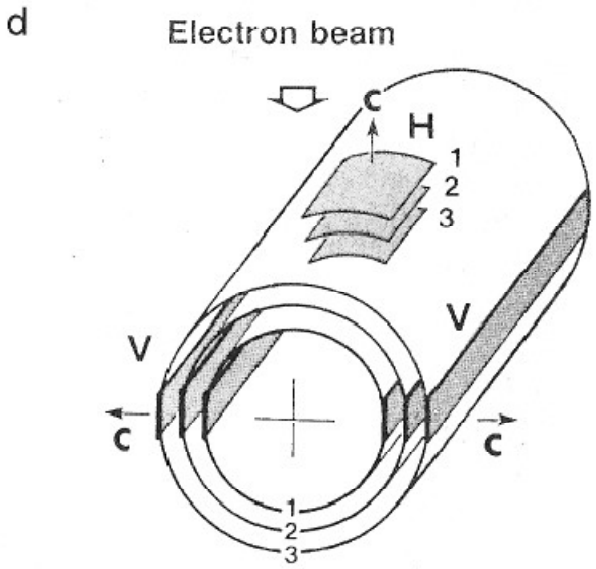

Fig. 19.3. The observation of N coaxial carbon tubules with various inner diameters d_i and outer diameters d_o reported by Iijima using TEM: (a) $N = 5$, $d_o = 67$ Å, (b) $N = 2$, $d_o = 55$ Å, and (c) $N = 7$, $d_i = 23$ Å, $d_o = 65$ Å. The sketch (d) indicates how the interference patterns for the parallel planes labeled H are used to determine the chiral angle θ, which in turn is found from the orientation of the tubule axis relative to the nearest zigzag axis defined in Fig. 19.2(a). The interference patterns that are labeled V determine the interplanar distances [19.1].

MWNTs :

Coaxially stacked cylinders !

Not Scroll-like tubes !

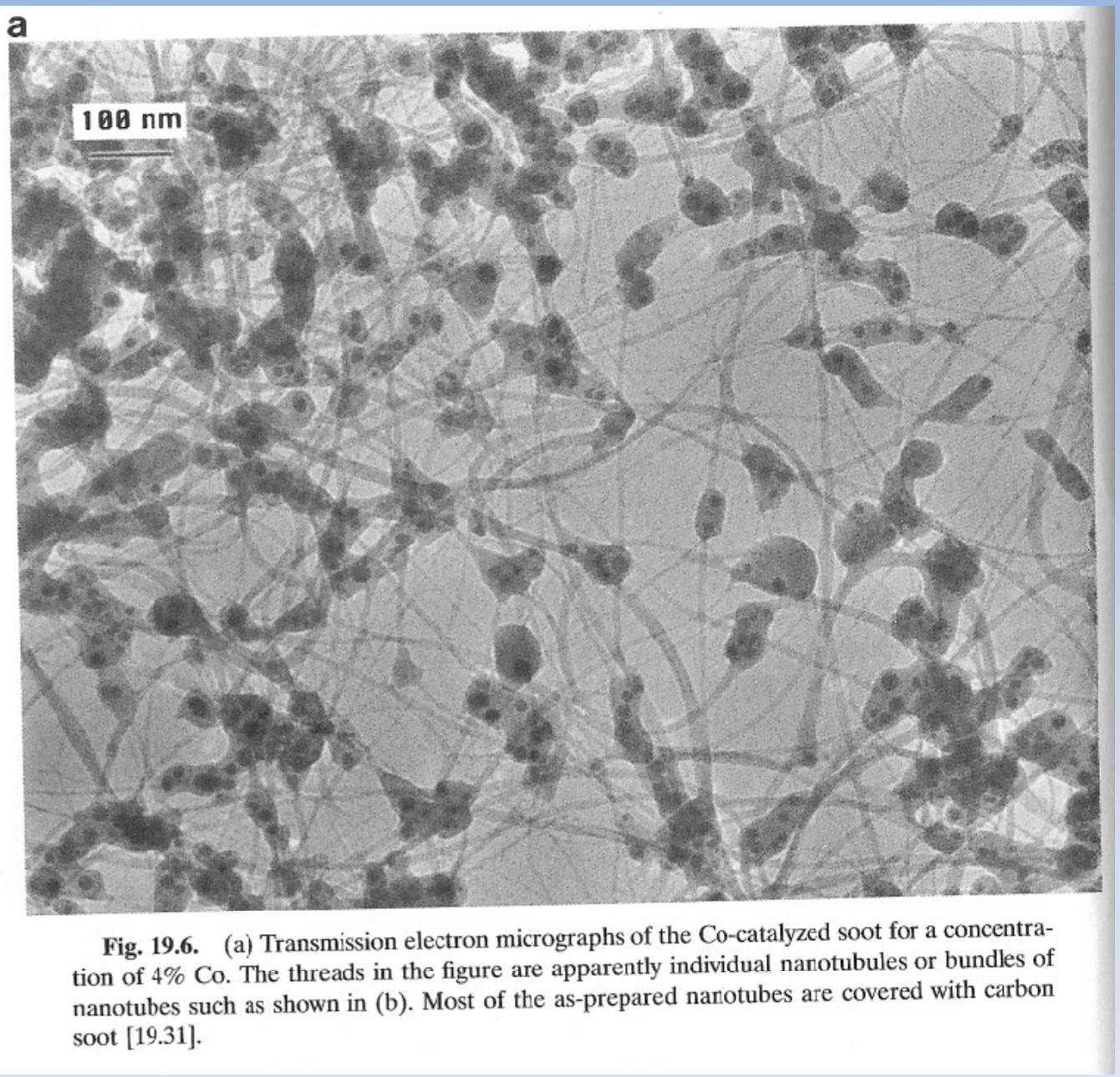

Fig. 19.6. (a) Transmission electron micrographs of the Co-catalyzed soot for a concentration of 4% Co. The threads in the figure are apparently individual nanotubules or bundles of nanotubes such as shown in (b). Most of the as-prepared nanotubes are covered with carbon soot [19.31].

Single-Walled NTs (SWNTs):

Co catalyst particles found at the ends of the tubes

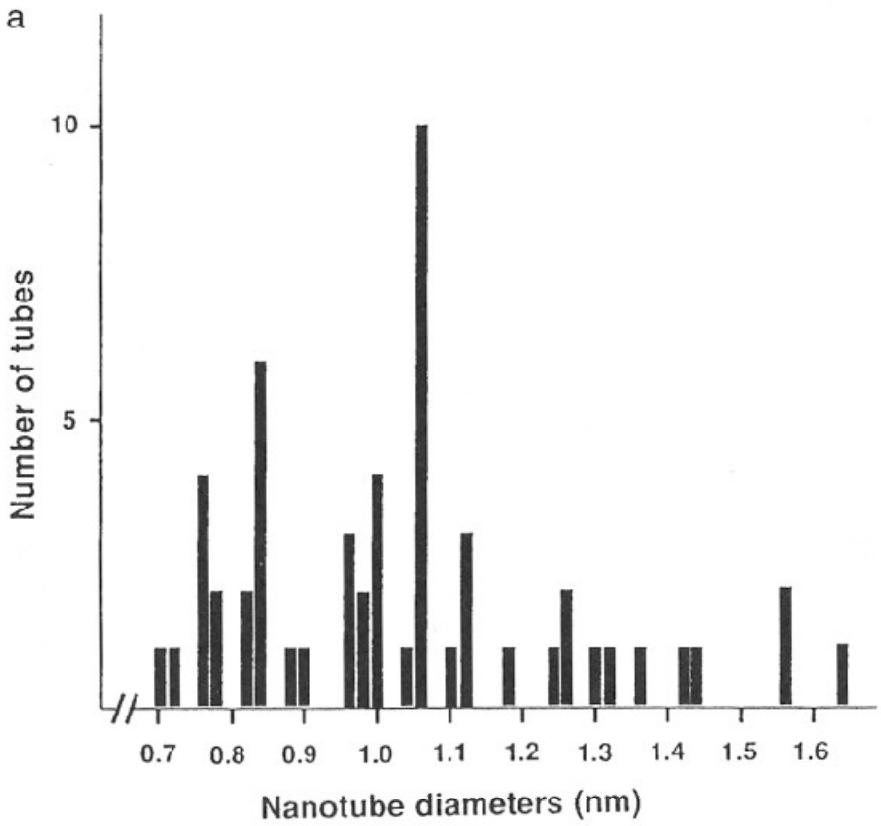

Fig. 19.8. Histograms of the single-wall nanotube diameter distribution for (a) Fe-catalyzed nanotubes [19.33] and (b) Co (4%)-catalyzed nanotubes [19.31].

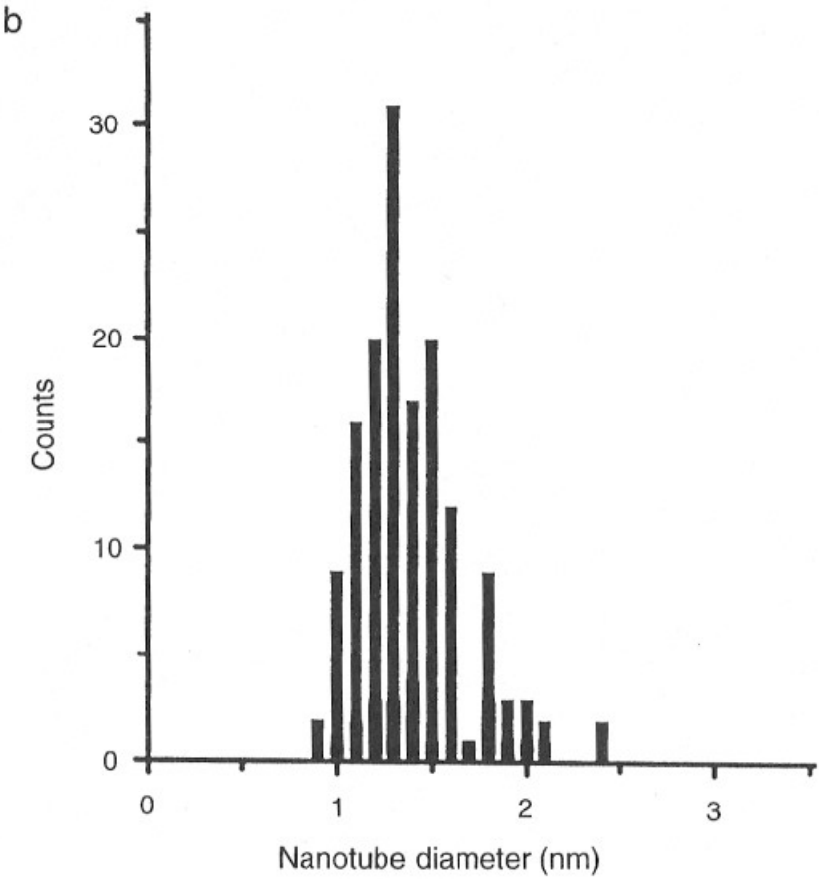

Fig. 19.8. (Continued).

Type of catalyst can result in different SWNTs size distribution

"Breathing" modes of carbon nanotube

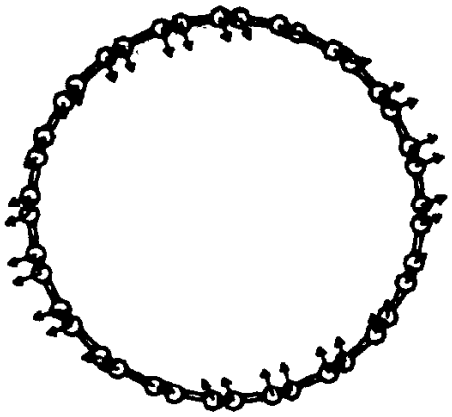

E_{2g} 17 cm^{-1}

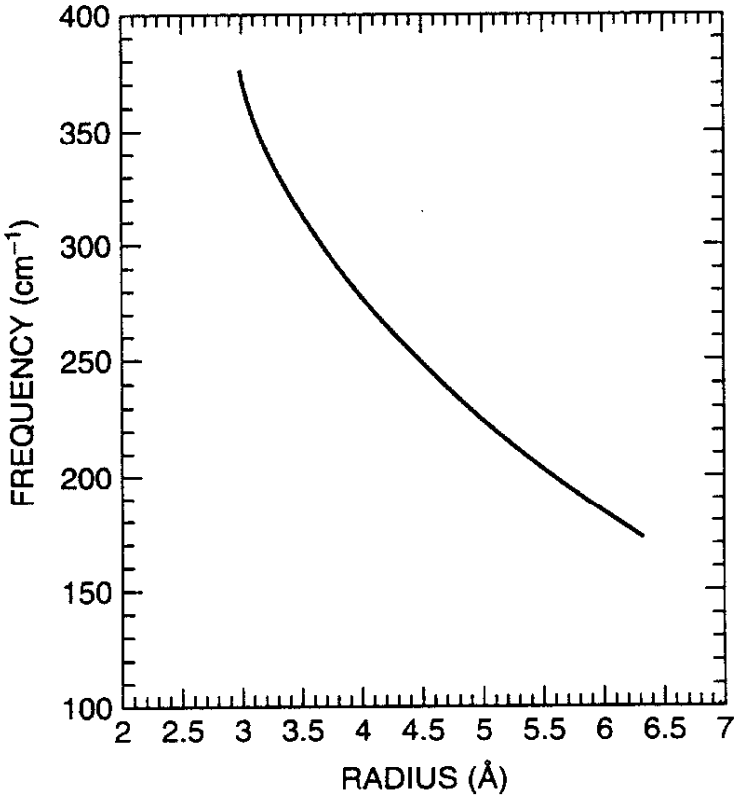

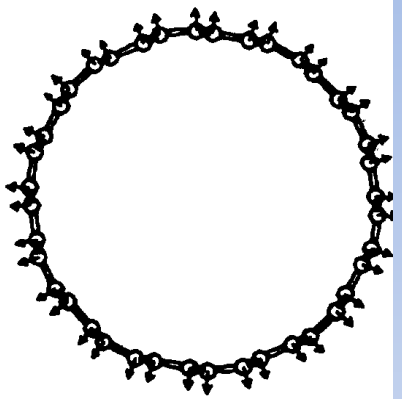

A_{1g} 165 cm^{-1}

Figure 5.20. Plot of the frequency of the Raman A_{1g} vibrational normal mode versus the radius of the nanotube. (10 Å = 1 nm). (Adapted from R. Saito, G. Dresselhaus, and M. S. Dresselhaus, *Physical Properties of Nanotubes*, Imperial College Press, 1998.)

SWNT stiffness is larger for smaller tube : higher elastic (strain) energy

Alternative way to determine the SWNT diameter d_t

Electronic property of carbon nanotube

Rolling of a 2-D graphene sheet

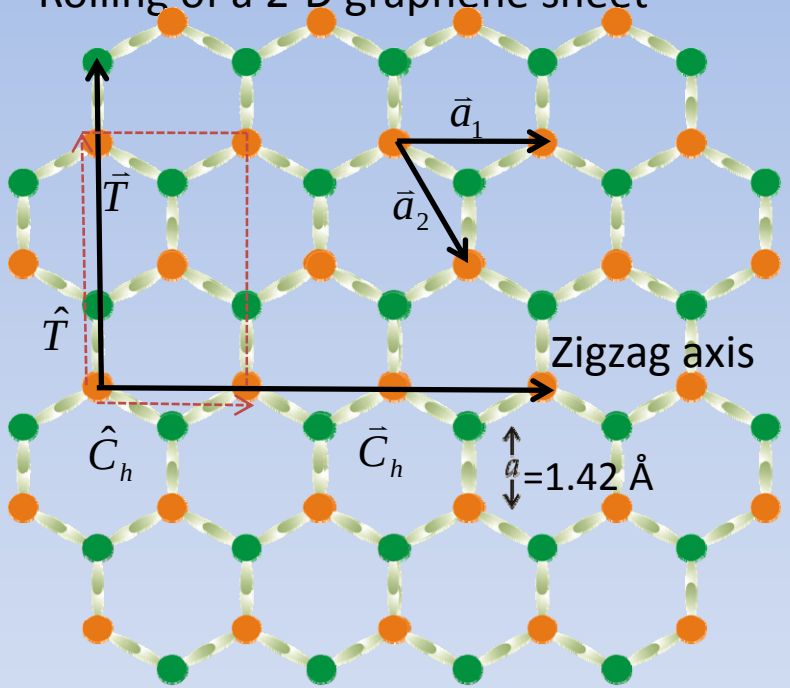

$$|\vec{a}_1| = |\vec{a}_2| \equiv a_0 = \sqrt{3} \times a_{cc}$$

Lattice vector for a 1-D CNT (n,m):

$$\hat{C}_h = \frac{a_0}{2d_R}(\sqrt{3}(n+m),(n-m)),$$

$$\hat{T} = \frac{\sqrt{3}a_0}{2d_R}(-(n-m),\sqrt{3}(n+m))$$

$$d_R = \begin{cases} 3d & \text{if (n - m) is a multiple of 3d} \\ d & \text{otherwise} \end{cases}$$

, where d is the highest common divisor of (n,m).

example: For (3,0) , $d_R = 3$

Reciprocal lattice vector for a 1-D CNT (n,m):

$$\vec{b}_1 = \frac{2\pi}{Na_0}(\sqrt{3}(n+m),(n-m)),$$

$$\vec{b}_2 = \frac{2\pi}{\sqrt{3}Na_0}(-(n-m),\sqrt{3}(n+m))$$

$$R_i \cdot b_j = 2\pi\delta_{ij}$$

$$N \equiv \frac{2(m^2+n^2+nm)}{d_R}, \text{ \# of hexagons per } \hat{T}.$$

Table 19.2

Values for characterization parameters[a] for selected carbon nanotubes labeled by (n, m) [19.5, 82].

(n,m)	d	d_R	d_t (Å)	L/a_0	T/a_0	N	$\psi/2\pi$	τ/a_0	Ω/d
(4, 2)	2	2	4.14	5	$\sqrt{21}$	28	5/28	$\sqrt{21}/14$	5
(5, 5)	5	15	6.78	$\sqrt{75}$	1	10	1/10	1/2	1
(9, 0)	9	9	7.05	9	$\sqrt{3}$	18	−1/18	$\sqrt{3}/2$	−1
(6, 5)	1	1	7.47	$\sqrt{91}$	$\sqrt{273}$	182	149/182	$\sqrt{3/364}$	149
(7, 4)	1	3	7.55	$\sqrt{93}$	$\sqrt{31}$	62	17/62	$1/\sqrt{124}$	17
(8, 3)	1	1	7.72	$\sqrt{97}$	$\sqrt{291}$	194	71/194	$\sqrt{3/388}$	71
(10, 0)	10	10	7.83	10	$\sqrt{3}$	20	−1/20	$\sqrt{3}/2$	−1
(6, 6)	6	18	8.14	$\sqrt{108}$	1	12	1/12	1/2	1
(10, 5)	5	5	10.36	$\sqrt{175}$	$\sqrt{21}$	70	1/14	$\sqrt{3/28}$	5
(20, 5)	5	15	17.95	$\sqrt{525}$	$\sqrt{7}$	70	3/70	$1/(\sqrt{28})$	3
(30, 15)	15	15	31.09	$\sqrt{1575}$	$\sqrt{21}$	210	1/42	$\sqrt{3/28}$	5
⋮	⋮	⋮	⋮	⋮	⋮	⋮	⋮	⋮	⋮
(n, n)	n	$3n$	$\sqrt{3}na/\pi$	$\sqrt{3}n$	1	$2n$	1/2n	1/2	1
$(n, 0)$	n	n	na/π	n	$\sqrt{3}$	$2n$	−1/2n	$\sqrt{3}/2$	−1

[a] Ω is given by Eq. (19.13); T is given by Eq. (19.7) with $a_0 = \sqrt{3}a_{C\text{-}C}$; L is the length of the chiral vector πd_t given by Eq. (19.2); N is given by Eq. (19.9); ψ is given by Eq. (19.12); τ is given by Eq. (19.11); Ω/d is the number of complete 2π revolutions about the tubule axis to reach a lattice point.

1-D Band structure for an armchair CNT (N_y,N_y):

2-D graphene sheet

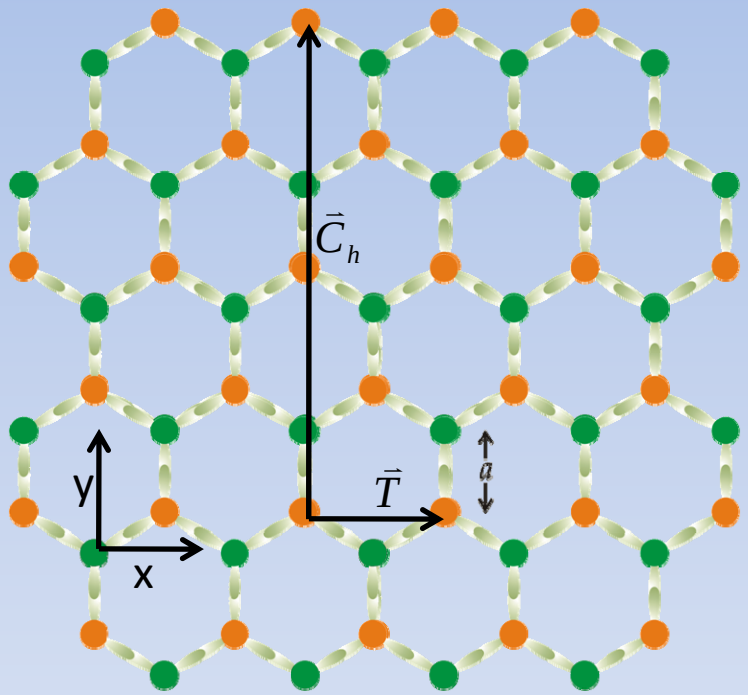

• Dispersion relation for 2D graphene :

$$E^{2D}(k_x, k_y) = \qquad \text{Eq(1)}$$

$$\pm t[1 + 4\cos(\frac{\sqrt{3}a}{2}k_x)\cos(\frac{3a}{2}k_y) + 4\cos^2(\frac{\sqrt{3}a}{2}k_x)]^{1/2}$$

Bohr-Sommerfeld quantization rule:

$$\int_{\substack{closed\\path}} p \cdot d\ell = qh \text{ , q is integer number}$$

• In 1D armchair CNT :

k_y satisfy periodic boundary condition

$$\boxed{\because k_y 3aN_y = 2\pi q}$$

$$\therefore E^{1D}{}_{arm}(k_x = k)$$

$$= \sum_{q=1}^{N_y} \pm t[1 \pm 4\cos(\frac{\sqrt{3}a}{2}k)\cos(\frac{\pi q}{N_y}) + 4\cos^2(\frac{\sqrt{3}a}{2}k)]^{1/2}$$

$$-\frac{\pi}{2} \le \frac{\sqrt{3}a}{2}k \le \frac{\pi}{2}$$

Example : 1-D Band structure for a armchair CNT (5,5):

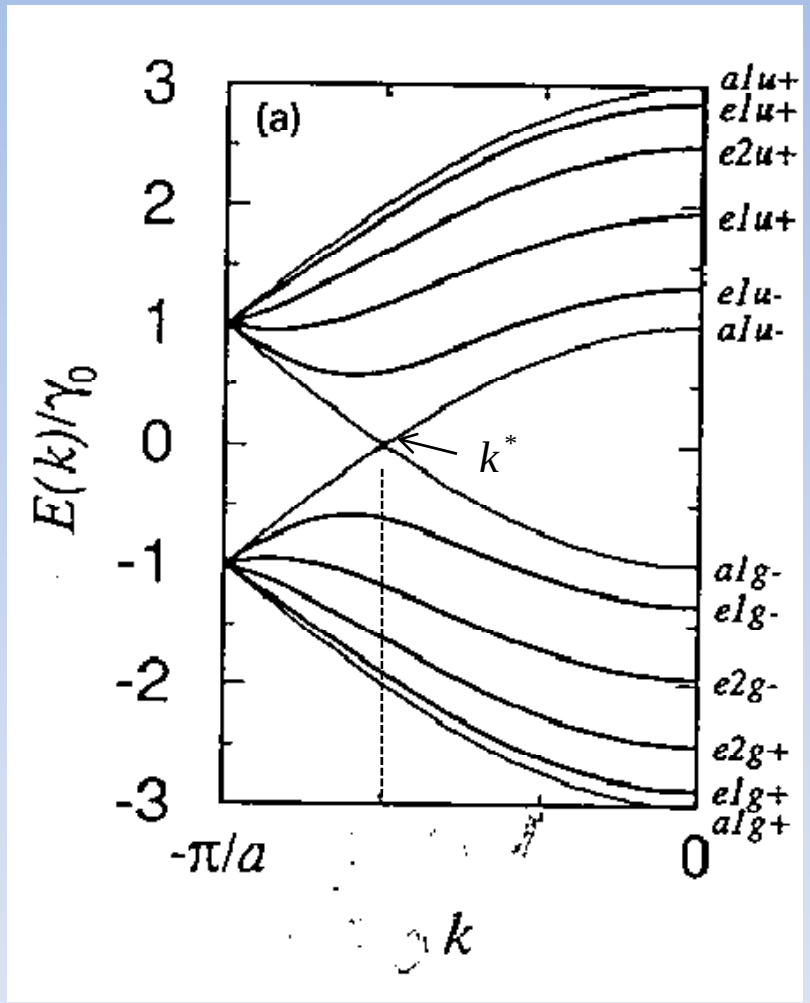

$$\therefore E^{1D}{}_{arm}(k_x = k, k_y = 2\pi q/15a)$$

$$= \sum_{q=1}^{5} \pm t[1 \pm 4\cos(\frac{\sqrt{3}a}{2}k)\cos(\frac{q\pi}{5}) + 4\cos^2(\frac{\sqrt{3}a}{2}k)]^{1/2}$$

$$-\frac{\pi}{2} \le \frac{\sqrt{3}a}{2}k \le \frac{\pi}{2}$$

- Conduction bands and valence bands each has
  4 doubly degenerate bands
  2 non-degenerate bands

- Band cross at k* : metallic conduction

$$\boxed{k^* = (\frac{2\pi}{3\sqrt{3}a}, \frac{2\pi}{3a})}$$

One of the Dirac point in 2-D band !!

1-D Band structure for a zigzag CNT (N_x,0):

2-D graphene sheet

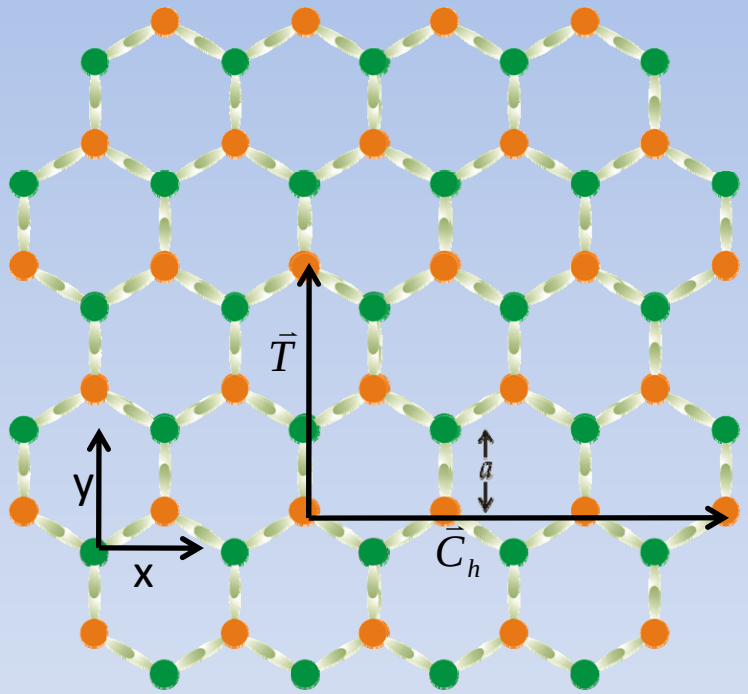

- In 1D zigzag CNT :

  k_x satisfy periodic boundary condition

$$\because k_x \sqrt{3} a N_x = 2\pi q$$

$$\therefore E^{1D}{}_{zigzag}(k_y = k)$$

$$= \sum_{q=1}^{N_x} \pm t[1 \pm 4\cos(\frac{3a}{2}k)\cos(\frac{q\pi}{N_x}) + 4\cos^2(\frac{q\pi}{N_x})]^{1/2}$$

$$-\frac{\pi}{2} \le \frac{3a}{2}k \le \frac{\pi}{2}$$

Example ： 1-D Band structure for a zigzag CNT (9,0):

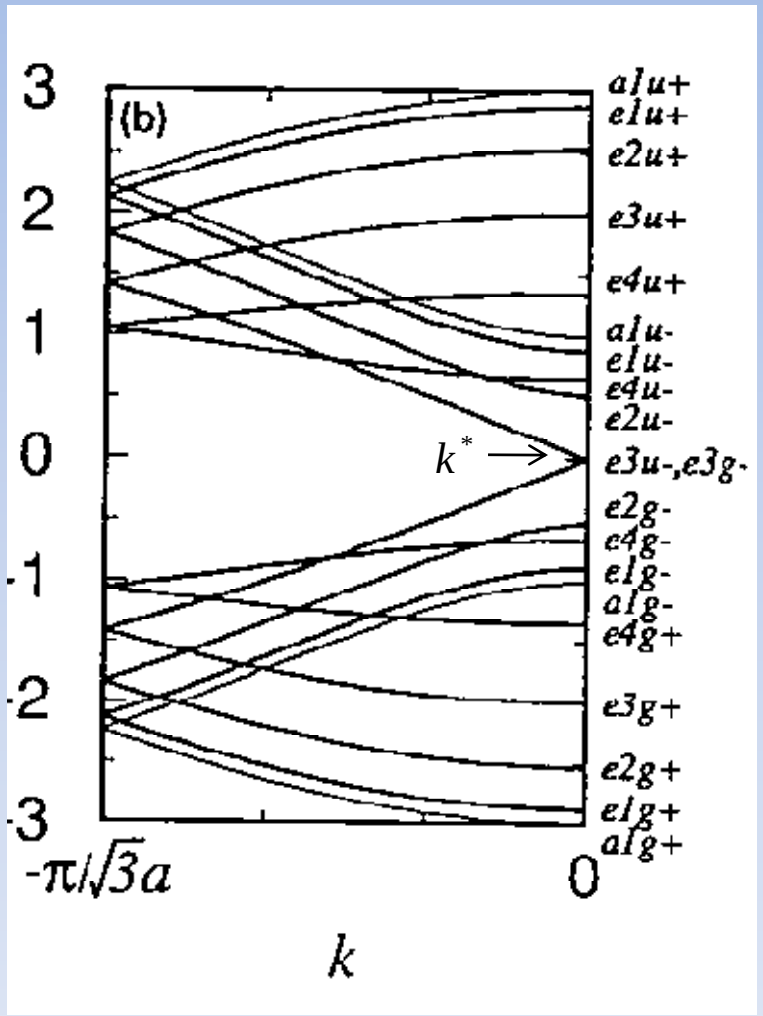

$$\therefore E^{1D}{}_{zigzag}(k_x = 2\pi q/9\sqrt{3}a, k_y = k)$$

$$= \sum_{q=1}^{9} \pm t[1 \pm 4\cos(\frac{3a}{2}k)\cos(\frac{q\pi}{9}) + 4\cos^2(\frac{q\pi}{9})]^{1/2}$$

$$-\frac{\pi}{2} \le \frac{3a}{2}k \le \frac{\pi}{2}$$

- Conduction bands and valence bands each has
  8 doubly degenerate bands
  2 non-degenerate bands

- Band cross at k* ： metallic conduction

$$\boxed{k^* = (\frac{4\pi}{3\sqrt{3}a}, 0)}$$

Another Dirac point in 2-D band !!

Example : 1-D Band structure for a zigzag CNT (10,0):

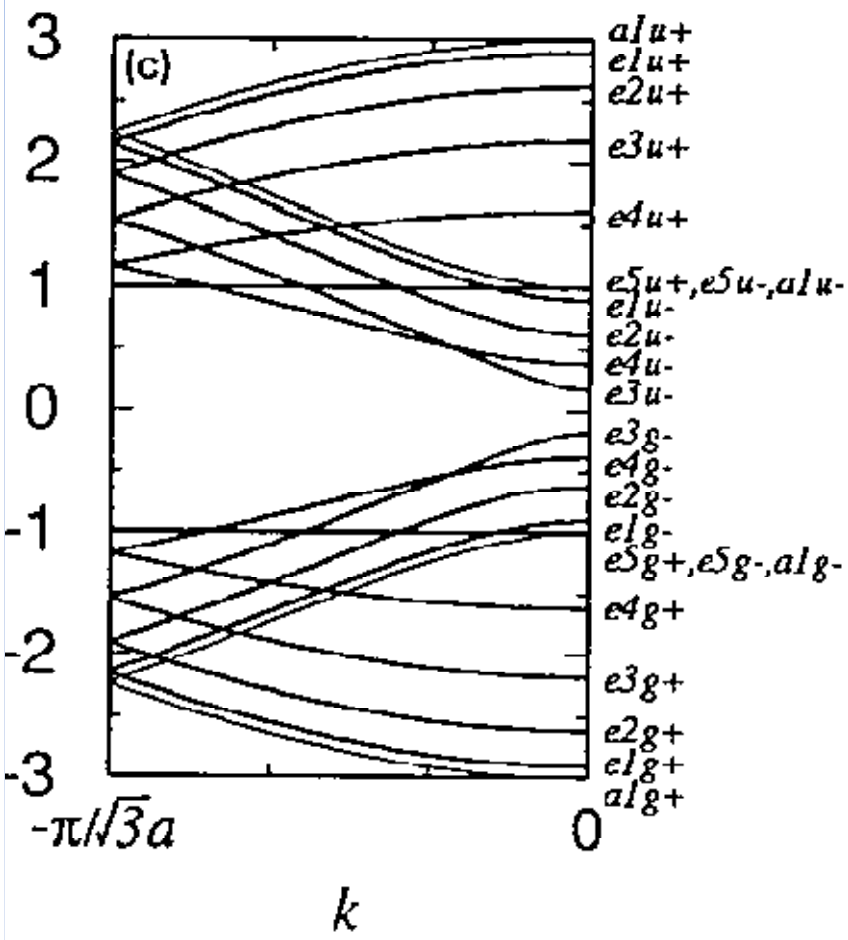

$$\therefore E^{1D}{}_{zigzag}\,(k_x = 2\pi q/10\sqrt{3}a, k_y = k)$$

$$= \sum_{q=1}^{10} \pm t[1 \pm 4\cos(\frac{3a}{2}k)\cos(\frac{q\pi}{10}) + 4\cos^2(\frac{q\pi}{10})]^{1/2}$$

$$-\frac{\pi}{2} \le \frac{3a}{2}k \le \frac{\pi}{2}$$

- Conduction bands and valence bands each has
  - 9 doubly degenerate bands
  - 2 non-degenerate bands
- No Band crossing : semiconducting transport !!

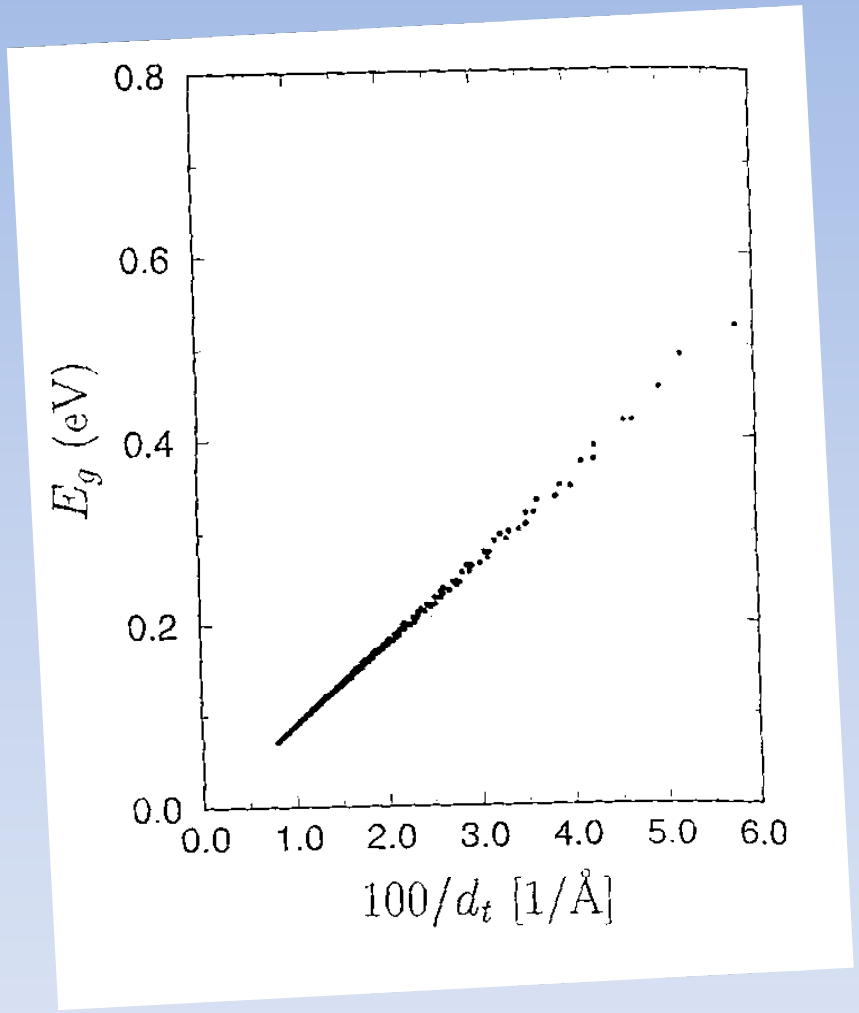

- Semiconducting CNTs:
  Band gap E_g depends on the tube diameter d_t, but independent of chiral angle θ

$$E_g = \frac{ta}{d_t} \propto \frac{1}{d_t}$$

Slicing a 2-D graphene band

- alternative way of looking at 1-D Band in CNT

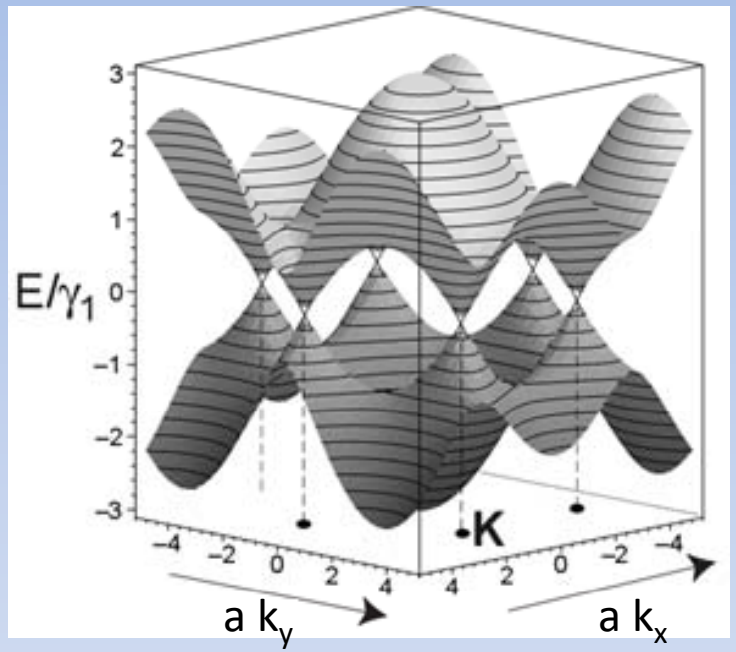

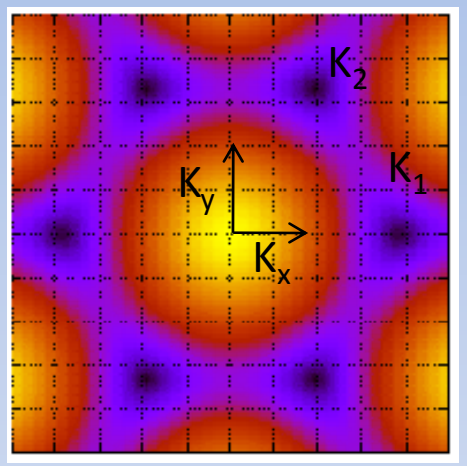

$$E(\vec{q} = \vec{K}) = 0$$

6 Dirac points

$$K_1 = \frac{4\pi}{3\sqrt{3}a}(1,0)$$

$$K_2 = \frac{4\pi}{3\sqrt{3}a}\left(\frac{1}{2}, \frac{\sqrt{3}}{2}\right)$$

- Whenever slicing through a Dirac point : metallic conduction
  otherwise : semiconducting transport behavior !

Armchair CNT (5,5):

$$\because k_y = \frac{2\pi q}{15a} \quad , -\frac{\pi}{\sqrt{3}a} \le k_x \le \frac{\pi}{\sqrt{3}a}$$

q=1,2…5

q=5

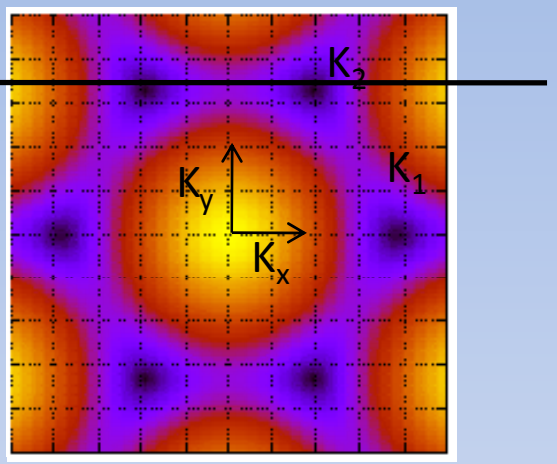

Slice through K_2 for q=5

➡ Metallic conduction

$$K_1 = \frac{4\pi}{3\sqrt{3}a}(1,0)$$

$$K_2 = \frac{4\pi}{3\sqrt{3}a}\left(\frac{1}{2}, \frac{\sqrt{3}}{2}\right)$$

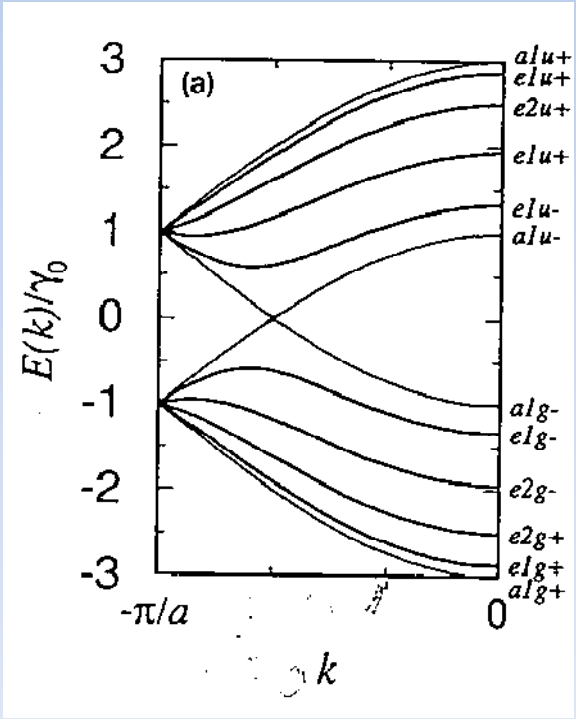

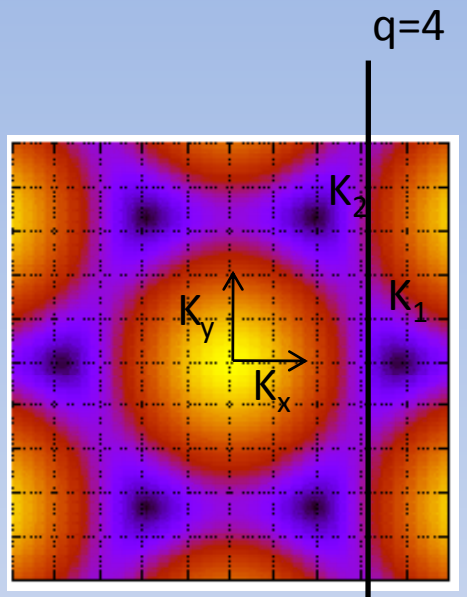

$$K_1 = \frac{4\pi}{3\sqrt{3}a}(1,0)$$

$$K_2 = \frac{4\pi}{3\sqrt{3}a}\left(\frac{1}{2},\frac{\sqrt{3}}{2}\right)$$

Zigzag CNT (10,0):

$$\because k_x = \frac{\pi q}{5\sqrt{3}a} \quad , -\frac{\pi}{3a} \le k_y \le \frac{\pi}{3a}$$

q=1,2…10

Does not Slice through any Dirac points

➡ Semiconducting transport behavior

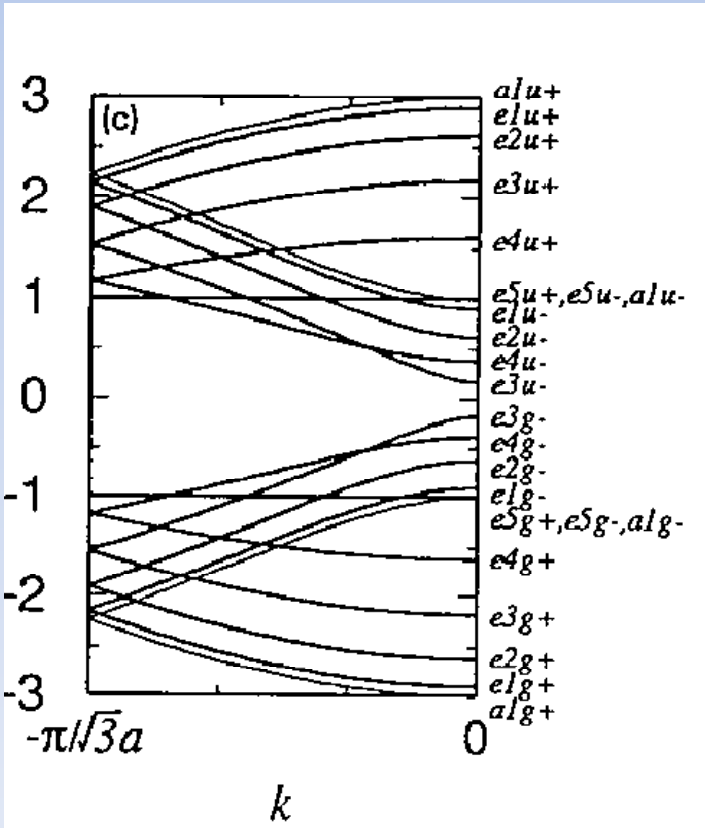

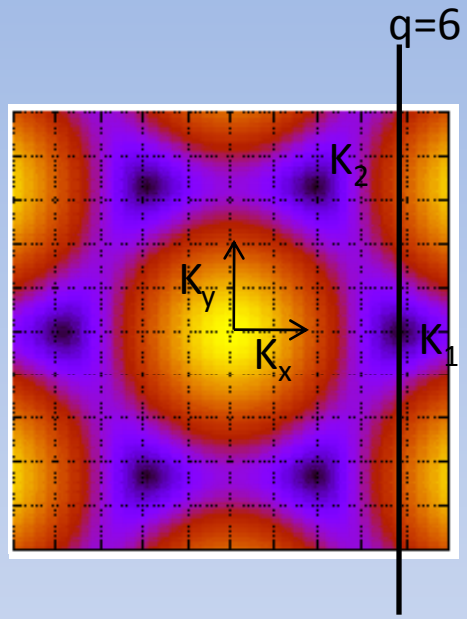

Zigzag CNT (9,0):

$$\because k_x = \frac{2\pi q}{9\sqrt{3}a} \quad , -\frac{\pi}{3a} \le k_y \le \frac{\pi}{3a}$$

q=1,2…9

Slice through K_1 for q=6

⇒ Metallic conduction

$$K_1 = \frac{4\pi}{3\sqrt{3}a}(1,0)$$

$$K_2 = \frac{4\pi}{3\sqrt{3}a}\left(\frac{1}{2}, \frac{\sqrt{3}}{2}\right)$$

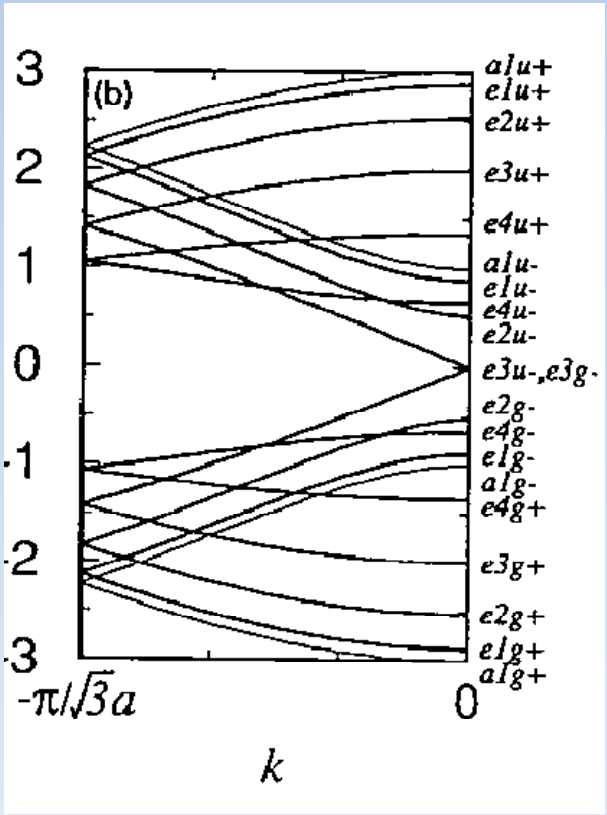

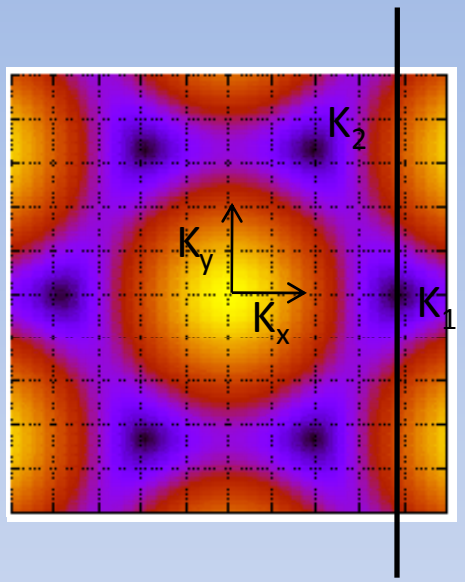

Zigzag CNT (N_x,0):

$$\because k_x = \frac{2\pi q}{N_x\sqrt{3}a}$$

q=1,2…N_x

- N_x : multiple of 3
  always Slice through K_1

⇒ 1/3 of Zigzag tube is metallic !!

$$K_1 = \frac{4\pi}{3\sqrt{3}a}(1,0)$$

$$K_2 = \frac{4\pi}{3\sqrt{3}a}\left(\frac{1}{2},\frac{\sqrt{3}}{2}\right)$$

In general, metallic for n-m = multiple of 3
Magic number “3” in CNTs !!

Triangular lattice

"Applications of carbon nanotube

- Field-effect transistor (FET)

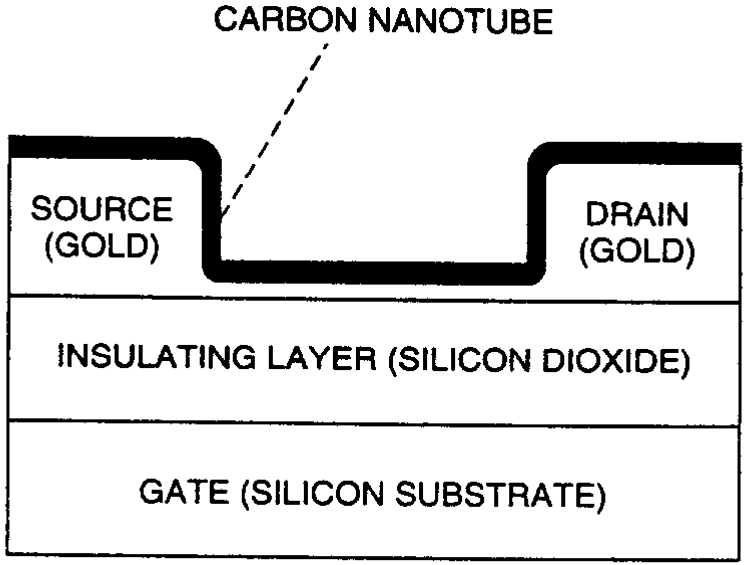

Figure 5.21. A schematic of a field-effect transistor made from a carbon nanotube.

Fast switching time and large field-effect on the conductivity of the CNTs

- CNT FET also as a chemical sensors

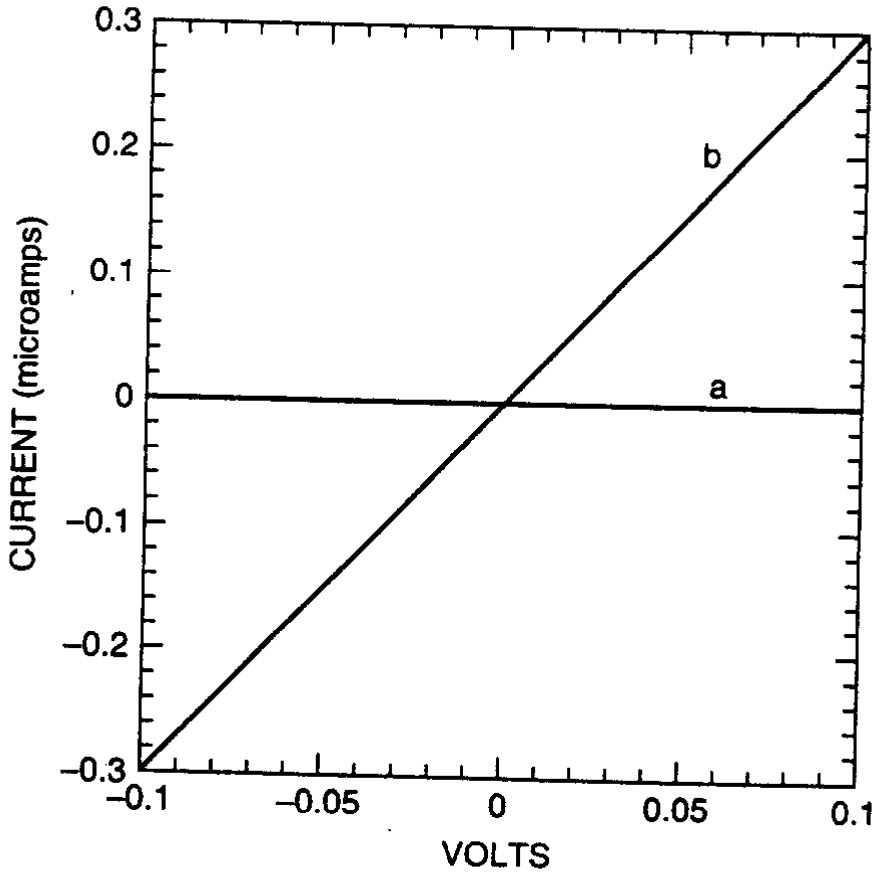

Figure 5.25. Plot of current versus voltage for carbon nanotube field effect transistor before (line a) and after (line b) exposure to NO_2 gas. These data were taken for a 4 V gate voltage. [Adapted from J. Kong et al., *Science* **287**, 622 (2000).]

- CNTs as a ions(Na^+, H^+) storage medium for Fuel cells

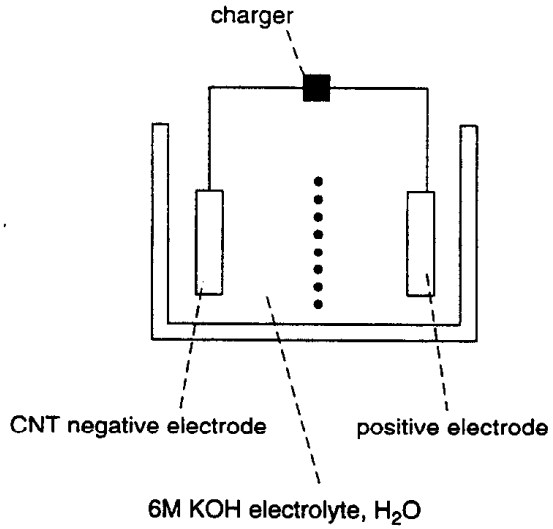

Figure 5.23. An electrochemical cell used to inject hydrogen into carbon nanotubes. The cell consists of an electrolytic solution of KOH with a negative electrode consisting of carbon nanotube (CNT) paper. Application of a voltage between the electrodes causes the H^+ ion to be attracted to the negative electrode. (Z. Iqbal, unpublished.)

Presence of H+ bonded to CNTs :
intensity reduction in Raman peaks

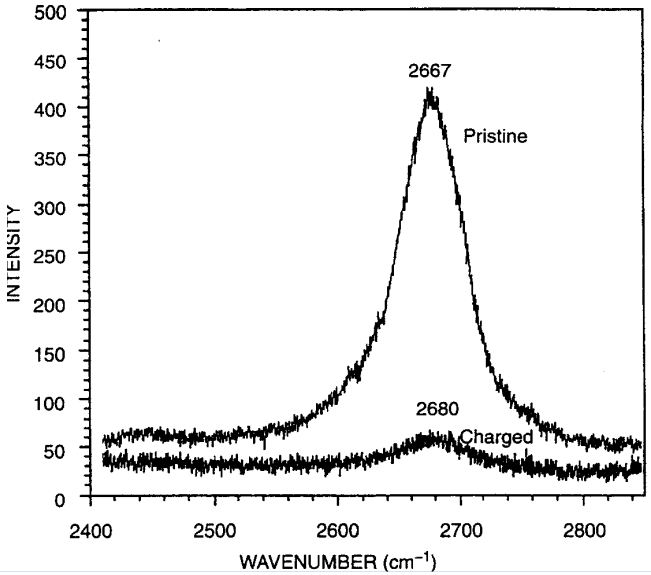

Figure 5.24. Raman spectrum of carbon nanotubes with peak intensity at 2667 cm^{-1} recorded before (pristine) and after (charged) treatment in the electrochemical cell sketched in Fig. 5.23. (From Z. Iqbal, unpublished.)

- CNTs as filler for mechanical reinforcement

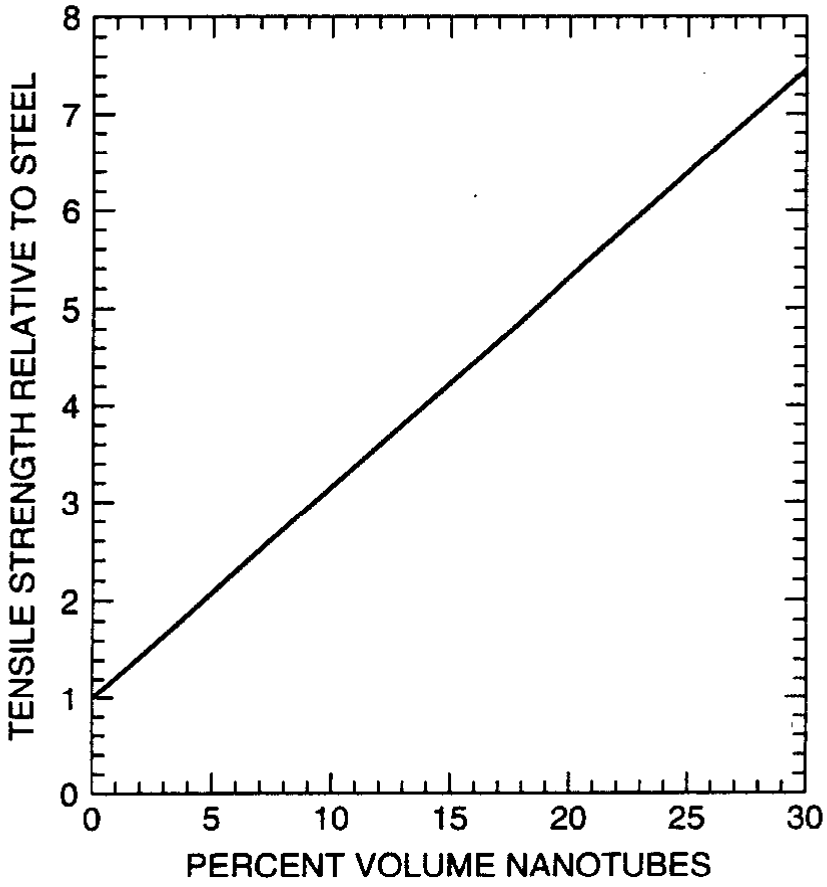

Figure 5.26. Tensile strength of steel versus volume fraction of carbon nanotubes calculated by the Kelly–Tyson formula. The nanotubes were 100 μm long and 10 nm in diameter.

carbon steel has higher tensile strength than regular steel

Concluding remark

- Label for a CNT (n,m)
- Mass production of CNTs using plasma enhanced CVD
- 1-D band structure of CNTs : slicing 2-D band structure of graphene
- 1/3 of the CNTs with random (n,m) is metallic.
- Application : CNT FETs, chemical sensors,
  Fuel cell storage medium, mechanical reinforcement